



Supplement of

Revealing joint evolutions and causal interactions in complex ecohydrological systems by a network-based framework

Lu Wang et al.

Correspondence to: Haiting Gu (ght000@zju.edu.cn) and Yue-Ping Xu (yuepingxu@zju.edu.cn)

The copyright of individual parts of the supplement might differ from the article licence.

S1 Introduction of Mann-Kendall test

The Mann-Kendall (MK) test searches for a trend in a series without specifying whether the trend is linear or nonlinear. Given a series $x(t)$ with the length of n , the null hypothesis of no trend assumes that the series $x(t)$ is independently distributed. The MK test is based on the test statistic S :

$$S = \sum_{i=1}^{n-1} \sum_{j=i+1}^n \text{sgn}(x(j) - x(i)) \quad (\text{Eq. S1.1})$$

with

$$\begin{cases} \text{sgn}(x) = 1 & \text{if } x > 0 \\ \text{sgn}(0) = 0 \\ \text{sgn}(x) = -1 & \text{if } x < 0 \end{cases} \quad (\text{Eq. S1.2})$$

A positive (negative) value of S indicates an upward (downward) trend. It is found that the statistic S is approximately normally distributed when $n > 8$. The standardized test statistic Z follows the standard normal distribution:

$$Z = \begin{cases} (S - 1) / \sqrt{\text{Var}(S)} & \text{if } S > 0 \\ \text{sgn}(0) = 0 \\ (S + 1) / \sqrt{\text{Var}(S)} & \text{if } S < 0 \end{cases} \quad (\text{Eq. S1.3})$$

The null hypothesis of no trend is rejected if the absolute value of Z is bigger than the theoretical value $Z_{1-\alpha/2}$, where α is the statistical significance level concerned.

S2 Datasets

Table S1. Brief description of datasets used in the study

| Type | Abbreviation | Variables | Data sources | Temporal resolution | Unit |
|--------------------------------------|--------------|--|--|---------------------|--------------|
| Hydrological variables | R | Runoff | National Hydrological Yearbook | Monthly | m^3/s |
| | SL | Sediment load | | | kg/s |
| | SMSA | Soil moisture storage anomaly | GLDAS-v2.1-Noah GRACE/GRACR-FO CSR | Monthly | mm |
| | SWSA | Surface water storage anomaly | | | mm |
| | TWSA | Terrestrial water storage anomaly | | | mm |
| | SCA | Snow cover area | MODIS-based snow cover product GRACE/GRACR-FO JPL | Monthly | km^2 |
| | NDVI | Normalized difference vegetation index | | | / |
| | GPP | Gross primary productivity | MOD17A2H.061 | Monthly | $gC\ m^{-2}$ |
| | WUE | Ecosystem water use efficiency | MOD17A2H.061 MOD16A2.061 | Monthly | $C/kg\ H_2O$ |
| Meteorological data (Auxiliary data) | P | Precipitation | | | mm |
| Human activity (Auxiliary data) | T | Temperature | China Meteorological Administration | Monthly | $^{\circ}C$ |
| | RSC | Reservoir storage change | National Hydrological Yearbook | Monthly | $10^8\ m^3$ |
| | WW | Water withdrawals | Water Resources Bulletin of the Yellow River | Annual | m^3 |

S3 Multi-year mean values of ecohydrological variables

Table S2. Multi-year mean values of eco-hydrological variables (in the growing season)

| Variables | R_modulus | TWSA | SMSA | GWSA | NDVI | GPP |
|-------------|---------------------------------------|--------------------------------------|---------------|---------|------------------|---------------------------------|
| Units | $\times 10^3 \text{ m}^3/\text{km}^2$ | mm | mm | mm | / | $\text{g}^*\text{C}/\text{m}^2$ |
| Region I | 84.98 | 5.15 | 12.87 | -7.84 | 0.45 | 339.95 |
| Region II | 84.39 | -1.65 | 4.28 | -5.58 | 0.49 | 476.17 |
| Region III | -57.36 | -22.18 | 2.88 | -24.79 | 0.27 | 260.19 |
| Region IV | - | -31.56 | 4.39 | -35.71 | 0.22 | 219.51 |
| Region V | 10.47 | -49.90 | 4.32 | -52.96 | 0.41 | 419.59 |
| Region VI | 13.64 | -42.48 | -8.08 | -32.85 | 0.55 | 632.47 |
| Region VII | 81.19 | -99.62 | -11.70 | -83.28 | 0.65 | 731.21 |
| Region VIII | -217.58 | -152.81 | -34.91 | -117.67 | 0.59 | 623.75 |
| Variables | WUE | SL_modulus | SCA | P | T | ET |
| Units | $\text{C}/\text{kg H}_2\text{O}$ | $\times 10^3 \text{ kg}/\text{km}^2$ | km^2 | mm | $^\circ\text{C}$ | mm |
| Region I | 0.98 | 66.94 | 7900 | 449.64 | 7.3 | 346.2 |
| Region II | 1.57 | 21.09 | | 400.74 | 11.7 | 302.59 |
| Region III | 1.86 | 105.42 | | 229.08 | 18.3 | 139.80 |
| Region IV | 2.02 | - | | 276.84 | 18.4 | 108.54 |
| Region V | 2.14 | 601.29 | | 407.88 | 18.8 | 194.82 |
| Region VI | 1.98 | 741.25 | | 442.92 | 19.3 | 318.96 |
| Region VII | 2.05 | -3778.52 | | 521.22 | 21.4 | 356.61 |
| Region VIII | 1.75 | 2307.59 | | 930.18 | 20.0 | 356.29 |

S4 Evolution trend of snow cover area

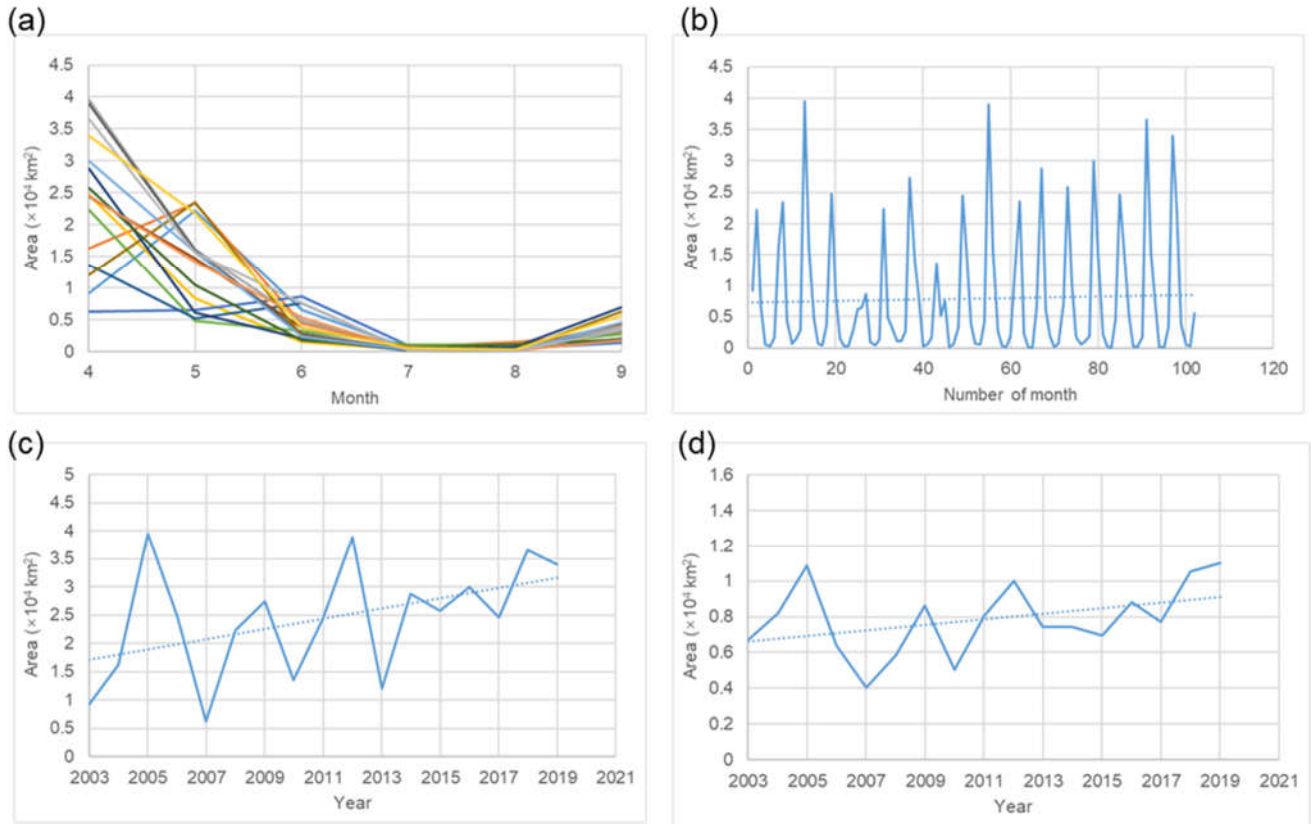


Figure S1. SCA during 2003-2019 in the source region of the YRB. (a) The intra-annual variation; (b) The monthly data. (c) The inter-annual variation (April). (d) The inter-annual variation (growing season average).

S5 Construction of correlation-based networks using different thresholds

For comparison, Pearson's correlation coefficient ($PCC>0.4$) and $PCC>0.5$ are also used as thresholds here. Although the existence of some links changes when different thresholds are used, the conclusions of the study remain unchanged. Overall, from the upper to the lower reaches, the modularity (M value) of the synchronous relationships increases (except for the downstream area) and the synchronization between the ecological and hydrological subsystems generally (S value) decreases.

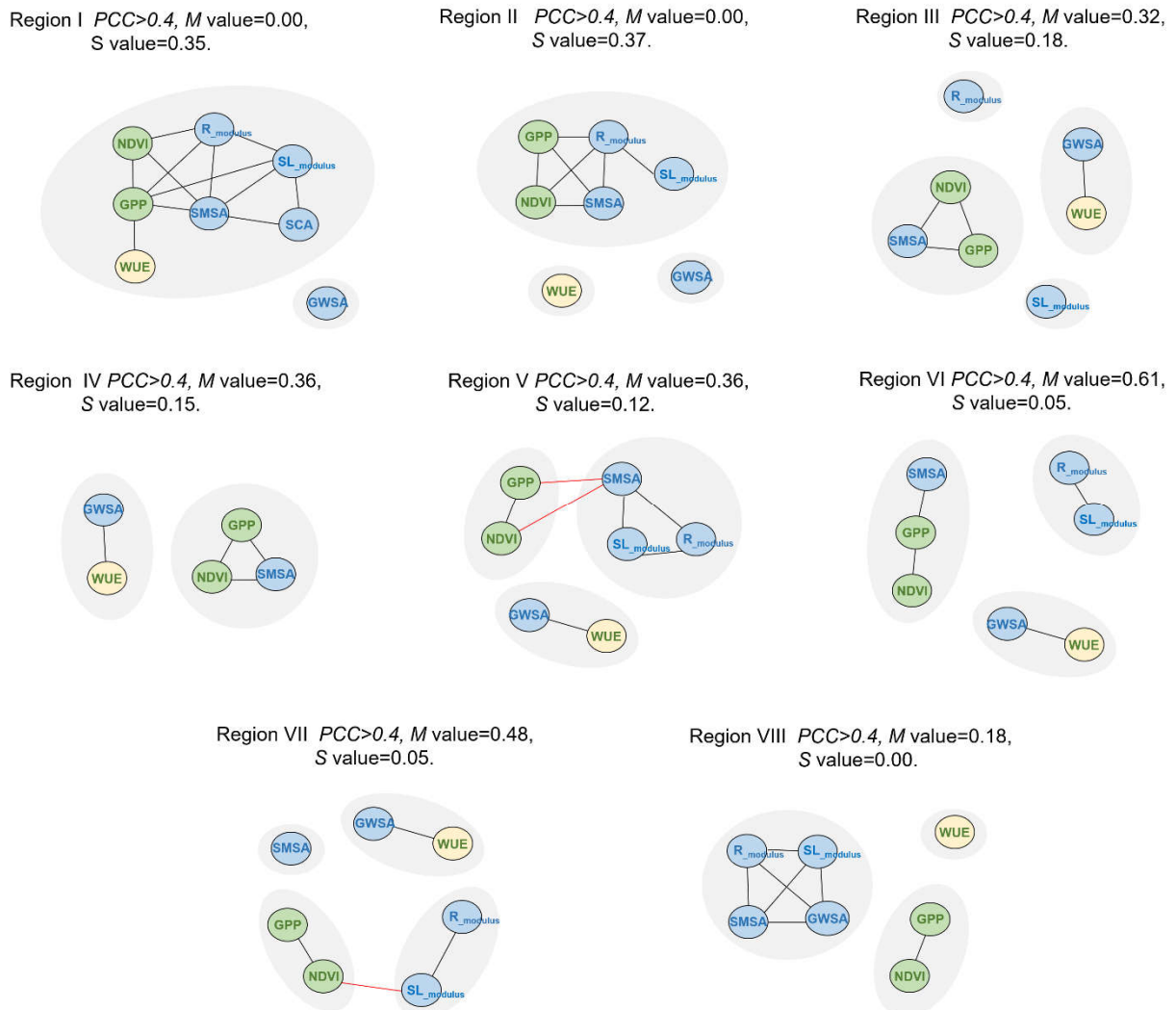


Figure S2. Synchronous networks and corresponding clustered modules (when $PCC>0.4$).

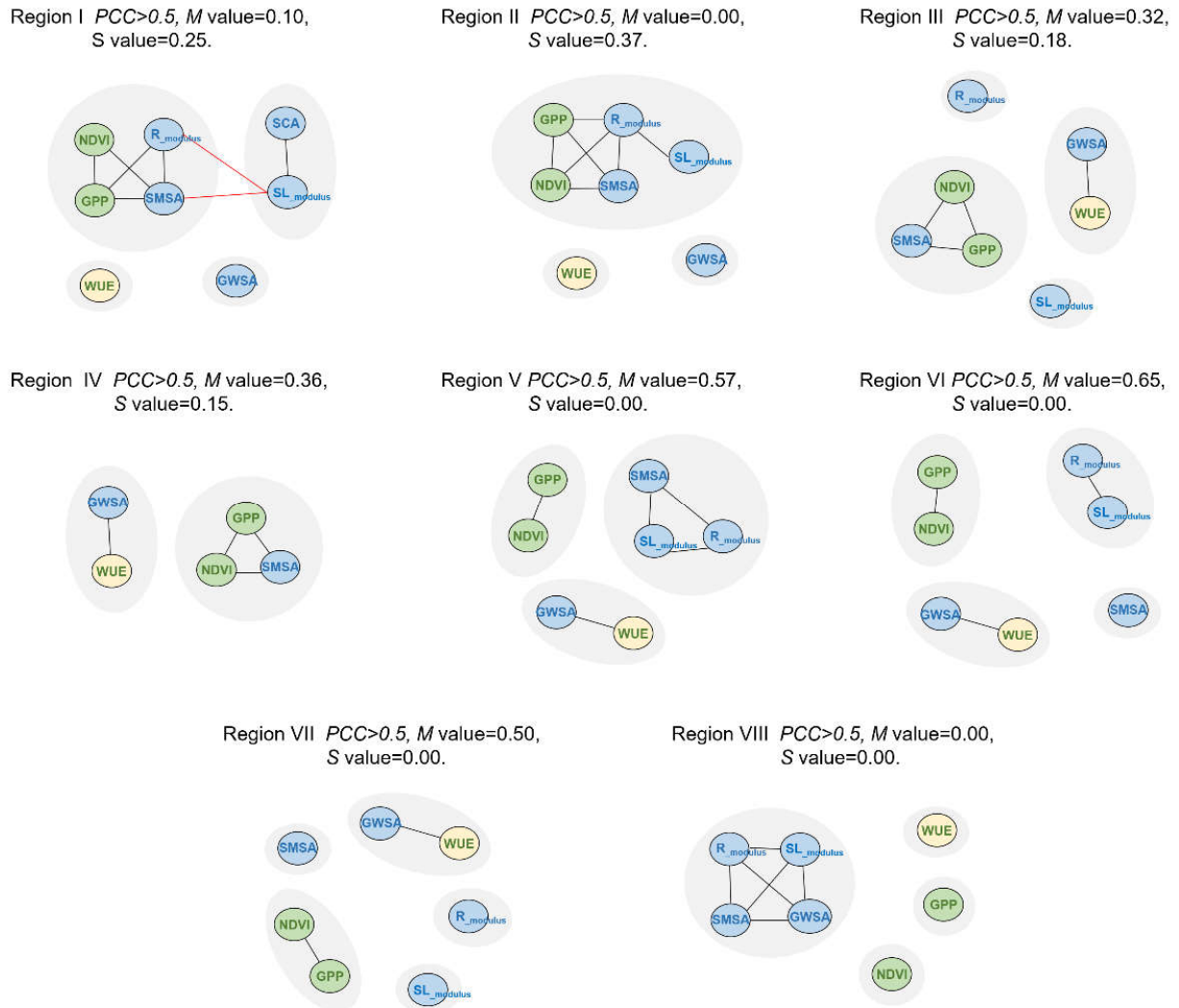


Figure S3. Synchronous networks and corresponding clustered modules (when $PCC>0.5$).

S6 Self-dependency in eco-hydrological variables

Table S3. The strength of self-dependency (if significant)

| Variable <i>i</i> | Variable <i>j</i> | Time lag of <i>i</i> | Link type <i>i--j</i> | Link value | Variable <i>i</i> | Variable <i>j</i> | Time lag of <i>i</i> | Link type <i>i--j</i> | Link value |
|----------------------|----------------------|-------------------------|--------------------------|---------------|----------------------|----------------------|-------------------------|--------------------------|---------------|
| Region I | | | | | Region V | | | | |
| \$R\$ | \$R\$ | 1 | --> | 0.23 | \$SMSA\$ | \$SMSA\$ | 1 | --> | 0.49 |
| \$SMSA\$ | \$SMSA\$ | 1 | --> | 0.59 | \$GWSA\$ | \$GWSA\$ | 1 | --> | 0.41 |
| \$GWSA\$ | \$GWSA\$ | 1 | --> | 0.62 | \$NDVI\$ | \$NDVI\$ | 1 | --> | 0.53 |
| \$NDVI\$ | \$NDVI\$ | 1 | --> | 0.33 | | | | | |
| \$GPP\$ | \$GPP\$ | 1 | --> | 0.24 | | | | | |
| \$GPP\$ | \$GPP\$ | 2 | --> | 0.24 | | | | | |
| \$ET\$ | \$ET\$ | 1 | --> | 0.42 | | | | | |
| Region II | | | | | Region VI | | | | |
| \$R\$ | \$R\$ | 1 | --> | 0.33 | \$R\$ | \$R\$ | 1 | --> | 0.28 |
| \$SL\$ | \$SL\$ | 1 | --> | 0.54 | \$SMSA\$ | \$SMSA\$ | 1 | --> | 0.47 |
| \$SMSA\$ | \$SMSA\$ | 1 | --> | 0.63 | \$GWSA\$ | \$GWSA\$ | 1 | --> | 0.39 |
| \$NDVI\$ | \$NDVI\$ | 1 | --> | 0.35 | \$NDVI\$ | \$NDVI\$ | 1 | --> | 0.51 |
| \$wue\$ | \$wue\$ | 1 | --> | 0.24 | \$RSC\$ | \$RSC\$ | 1 | --> | 0.34 |
| \$ET\$ | \$ET\$ | 1 | --> | 0.30 | | | | | |
| Region III | | | | | Region VII | | | | |
| \$SL\$ | \$SL\$ | 1 | --> | 0.54 | \$SMSA\$ | \$SMSA\$ | 1 | --> | 0.33 |
| \$SMSA\$ | \$SMSA\$ | 1 | --> | 0.42 | \$GWSA\$ | \$GWSA\$ | 1 | --> | 0.44 |
| \$GWSA\$ | \$GWSA\$ | 1 | --> | 0.35 | \$NDVI\$ | \$NDVI\$ | 1 | --> | 0.30 |
| \$NDVI\$ | \$NDVI\$ | 1 | --> | 0.29 | \$T\$ | \$T\$ | 1 | --> | 0.20 |
| | | | | | \$ET\$ | \$ET\$ | 1 | --> | 0.24 |
| Region IV | | | | | Region VIII | | | | |
| \$SMSA\$ | \$SMSA\$ | 1 | --> | 0.54383 | \$SMSA\$ | \$SMSA\$ | 1 | --> | 0.39 |
| \$GWSA\$ | \$GWSA\$ | 1 | --> | 0.48938 | \$GWSA\$ | \$GWSA\$ | 1 | --> | 0.46 |
| \$NDVI\$ | \$NDVI\$ | 1 | --> | 0.65776 | \$GPP\$ | \$GPP\$ | 1 | --> | 0.30 |
| \$ET\$ | \$ET\$ | 1 | --> | 0.38774 | \$ET\$ | \$ET\$ | 1 | --> | 0.29 |

S7 Link strength of GPP versus ET to WUE

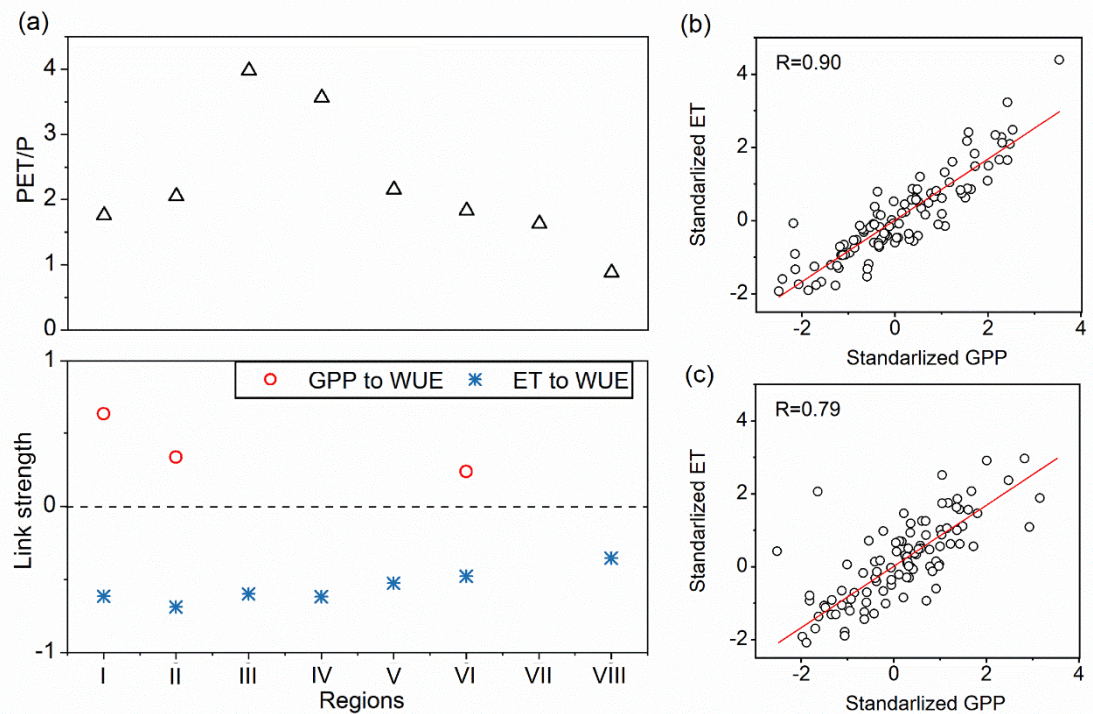


Figure S4. (a) Link strength of GPP versus ET to WUE in the eight subregions in the Yellow River basin. The top plot is the PET/P of each subregion, where the larger the value, the more arid the region. The figure only exhibits significant links. (b) Correlations of standardized ET versus GPP in Region VII. (c) Correlations of standardized ET versus GPP in Region VIII.

S8 Annual WUE evolutions across the YRB



Figure S5. Annual WUE evolutions during 2003-2019 across the eight subregions of the YRB.